

Strongly interacting Majorana fermions

Ching-Kai Chiu, D.I. Pikulin, and M. Franz

*Department of Physics and Astronomy, University of British Columbia, Vancouver, BC, Canada V6T 1Z1 and
Quantum Matter Institute, University of British Columbia, Vancouver BC, Canada V6T 1Z4*

(Dated: December 7, 2024)

Interesting phases of quantum matter often arise when the constituent particles – electrons in solids – interact strongly. Such strongly interacting systems are however quite rare and occur only in extreme environments of low spatial dimension, low temperatures or intense magnetic fields. Here we introduce a new system in which the fundamental electrons interact only weakly but the low energy effective theory is described by strongly interacting Majorana fermions. The system consists of an Abrikosov vortex lattice in the surface of a strong topological insulator and is accessible experimentally using presently available technology. The simplest interactions between the Majorana degrees of freedom exhibit an unusual nonlocal structure that involves four distinct Majorana sites. We formulate simple lattice models with this type of interaction and find exact solutions in certain physically relevant one- and two-dimensional geometries. In other cases we show how our construction allows for the experimental realization of interesting spin models previously only theoretically contemplated.

I. INTRODUCTION

When fermions partially occupy a band that is flat their kinetic energy is quenched and interactions, even when nominally weak, can have a profound effect on the ground state of the system. This paradigm is realized, with spectacular results, in 2D electron gases in perpendicular magnetic field where the interplay between the flat Landau level band structure and the Coulomb interaction gives rise to fractional quantum Hall effect (FQHE) with all its remarkable phenomenology^{1,2}. More recently, it has been realized that magnetic field is not necessary for the formation of FQHE states: one can obtain these, at least in principle, from lattice models that are tuned so that their conduction band is (nearly) flat and at the same time exhibits a non-zero Chern number making it topologically nontrivial^{3–8}. When these conditions are met one can achieve FQHE without magnetic field and there has been considerable interest in such systems recently. In practice, however, it is not clear how a lattice system with a topologically non-trivial flat band could be realized experimentally because the occurrence of a flat band typically requires considerable fine tuning of the overlap integrals which are given in solids by crystal chemistry and this is, in most cases, not continuously tunable. Proposals exist to artificially engineer such systems in optical lattices and dipolar spin systems^{9,10}.

In this study we introduce a physical lattice system in which a completely flat band can be obtained by tuning a single parameter. The band is unusual because its fundamental degrees of freedom are Majorana fermions. In the flat band regime the Hamiltonian is dominated by the interaction term and the system is therefore inherently strongly correlated. Its phenomenology differs substantially from the FQHE paradigm. Interesting phases nevertheless arise and we explore them in some detail.

The specific system we consider is depicted in Fig. 1 and consists of the Abrikosov lattice of vortices in the surface state of a strong topological insulator (STI) that has

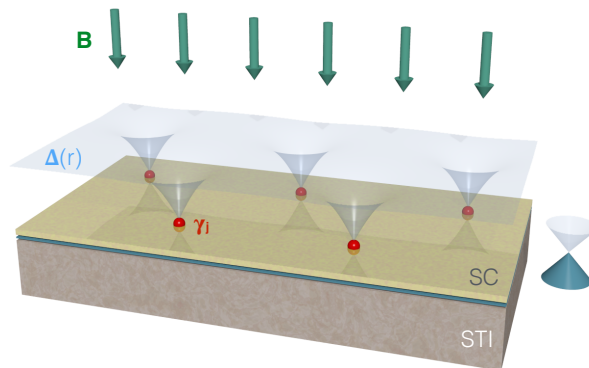


FIG. 1: **Schematic depiction of the system based on Fu-Kane model**¹⁸. Superconducting order is induced in the surface of a strong topological insulator (STI) gapping out the protected surface states with the Dirac dispersion. Magnetic field \mathbf{B} is then applied to induce Abrikosov vortices in the SC order parameter $\Delta(\mathbf{r})$. Each vortex hosts an unpaired Majorana zero mode γ_j .

been made superconducting, either intrinsically as suggested by recent experiments^{11,12}, or through the proximity effect with an adjacent ordinary superconductor^{13–17}. Theoretically, the situation is described by the Fu-Kane model¹⁸ which also famously predicts that each vortex in the SC order parameter binds a Majorana zero mode. Tentative experimental evidence for such zero modes has been recently reported in $\text{Bi}_2\text{Te}_3/\text{NbSe}_2$ heterostructures¹⁹.

When two vortices are brought together their Majorana wavefunctions start overlapping and, generically, the zero modes split. In the vortex lattice one thus expects formation of a Majorana band whose bandwidth increases as the lattice becomes denser and this is indeed observed in analytical and numerical calculations^{20–25}. However, in the special case the chemical potential μ of the STI coincides with the Dirac point of the surface state (hereafter referred to as the neutrality point) the band

formation can be avoided. The Fu-Kane model at the neutrality exhibits an extra ‘‘chiral’’ symmetry and, as observed by Teo and Kane²⁶, vortex defects are then in topological class BDI described by an integer (as opposed to Z_2 valued) invariant. Physically, this means that the total number of exact zero modes in the system is equal to the total vorticity, i.e. the total number N of vortices present in the system^{27–29}. This is to be contrasted with the Z_2 classification that applies away from the neutrality point and implies $(N \bmod 2)$ exact zero modes. We thus arrive at a conclusion that at the neutrality point the chiral symmetry present in the Fu-Kane model prohibits Majorana zero modes from hybridizing. The Majorana band that arises in the vortex lattice therefore remains completely flat. A small detuning $\delta\mu$ away from the neutrality point will produce a small bandwidth w proportional to $\delta\mu$. In appendix A we outline how this physics arises in a concrete model calculation.

II. INTERACTIONS IN MAJORANA FLAT BANDS

In the absence of hopping terms the leading perturbation to the degenerate manifold of Majorana zero modes will arise from electron-electron interactions that are necessarily present in the underlying solid. If we denote by γ_j the annihilation operator of the Majorana zero mode belonging to the j -th vortex then the simplest interaction term that can be constructed has the form

$$\mathcal{H}_{\text{int}} = \sum_{ijkl} g_{ijkl} \gamma_i \gamma_j \gamma_k \gamma_l, \quad (1)$$

where g_{ijkl} are real constants representing the interaction strength. The reality of g_{ijkl} follows from the requirement that \mathcal{H}_{int} be hermitian. Furthermore, since the Majorana operators obey the anticommutation algebra

$$\{\gamma_i, \gamma_j\} = 2\delta_{ij}, \quad \gamma_i^\dagger = \gamma_i, \quad (2)$$

only the part of g_{ijkl} that is antisymmetric in all indices contributes to \mathcal{H}_{int} . We note specifically that according to Eq. (2) $\gamma_i^\dagger \gamma_i = \gamma_i \gamma_i = 1$ and the terms in \mathcal{H}_{int} with two identical indices reduce to fermion hoppings, e.g. $g_{iikl} \gamma_i \gamma_i \gamma_k \gamma_l = g_{iikl} \gamma_k \gamma_l$. However, such terms are not hermitian and one can show that since $g_{iikl} = g_{iilk}$ they identically vanish. The simplest interaction term thus involves Majoranas located at four distinct vortices. Such a non-local interaction may be expected to give rise to unusual physical properties.

The expression in Eq. (1) is cumbersome because for every group of four vortices it contains 24 distinct permutations of the γ operators. It is thus preferable to rewrite \mathcal{H}_{int} as a sum over all distinct groups of four vortices in each of which we define a specific ordering of γ 's. For example for the group $(\gamma_1, \gamma_2, \gamma_3, \gamma_4)$ we write the interaction term as

$$\mathcal{H}_{\text{int}}^{1234} = g\gamma_1\gamma_2\gamma_3\gamma_4 \quad (3)$$

and similarly for other groups with γ 's organized in order of increasing index j . As demonstrated in appendix B the interaction strength g for every such group of four can be written as

$$g = \frac{1}{2} \epsilon^{ijkl} \int \int dr^2 dr'^2 \rho_{ij}(\mathbf{r}) V(\mathbf{r} - \mathbf{r}') \rho_{kl}(\mathbf{r}'), \quad (4)$$

where ϵ^{ijkl} is the totally antisymmetric tensor, $V(\mathbf{r} - \mathbf{r}')$ is the (screened) Coulomb interaction and $\rho_{ij}(\mathbf{r})$ denotes the charge density associated with Majorana zero modes at i and j . The latter is given in terms of the zero mode wavefunctions $\Phi_j(\mathbf{r})$, represented as four-component spinors in the combined Nambu and spin spaces.

The coupling strength g defined in Eq. (4) depends on the zero mode wavefunction overlaps as well as the detailed form of the interaction potential $V(\mathbf{r})$ and is generally difficult to precisely evaluate. For our purposes it will suffice to note that since $\Phi_j(\mathbf{r})$ decay exponentially outside the vortex core, the largest g will occur for those groups of four vortices that are packed closest together. In the following we shall consider examples of lattice systems in which we retain only such dominant interactions and neglect all g 's associated with groups of vortices that are more spread out since they are smaller by factors $\sim e^{-d/\xi}$ where d is the intervortex distance and ξ the SC coherence length. For instance in the square vortex lattice we shall retain g_{\square} associated with an elementary square plaquette and neglect all other couplings.

In addition to the dominant four-fermion term we shall often consider small hopping terms that may arise from a weak detuning away from the neutrality point. As discussed in Ref.³⁰ such hopping terms can be written as

$$\mathcal{H}_{\text{kin}} = \sum_{i,j} t_{ij} s_{ij} \gamma_i \gamma_j, \quad (5)$$

where t_{ij} is a real symmetric matrix representing the hopping strength while $s_{ij} = e^{i\phi_{ij}} = \pm i$ are the Z_2 gauge factors. The latter arise from the fact that one can perform a local Z_2 gauge transformation $\gamma_j \rightarrow -\gamma_j$ without affecting the zero mode commutation algebra (2). A product of s_{ij} factors along a closed trajectory however is gauge invariant and physically observable. In the vortex lattice for a general polygon formed by n vortices the total phase is given by³⁰

$$\sum_{\text{polygon}} \phi_{ij} = \frac{\pi}{2}(n-2). \quad (6)$$

III. LATTICE MODELS WITH INTERACTING MAJORANA FERMIONS

We now proceed to study specific interacting models in one and two dimensions. We focus on lattice geometries whose building blocks are square plaquettes because

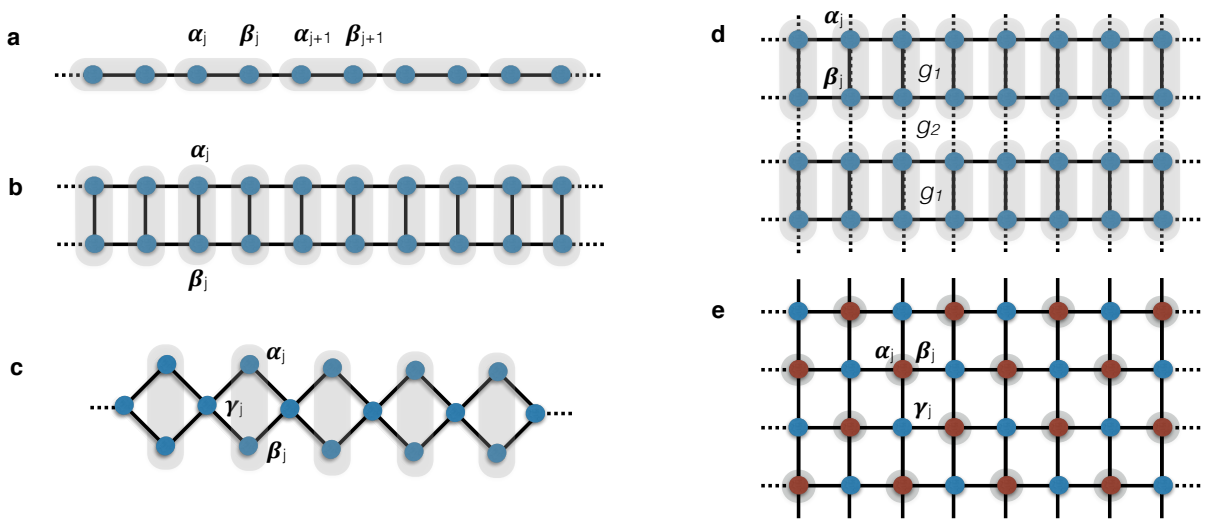


FIG. 2: Lattice structures for models with strongly interacting Majorana fermions. **a** Simple 1D chain, **b** two-leg ladder and **c** the diamond chain. **d** Simple square lattice with two types of plaquettes characterized by interaction strength g_1 and g_2 and **e** the modified square lattice with alternate sites (rendered in red) occupied by double vortices.

they naturally accommodate the four-fermion interaction terms (1). We begin with 1D structures which can be physically realized by inducing SC order in a narrow strip on the surface of an STI and then applying magnetic field of appropriate strength perpendicular to the surface.

A simple *linear chain* depicted in Fig. 2a is described by an interacting Hamiltonian of the form

$$\mathcal{H}_{\text{int}} = g_1 \sum_j \alpha_j \beta_j \alpha_{j+1} \beta_{j+1} + g_2 \sum_j \beta_j \alpha_{j+1} \beta_{j+1} \alpha_{j+2}. \quad (7)$$

Here α_j and β_j denote two Majoranas in the two site unit cell j . In a uniform chain $g_1 = g_2$ but we consider here a more general case of dimerized bond lengths leading to alternating couplings g_1 and g_2 . The Hamiltonian (7) can be brought to a more familiar form by performing a Wigner-Jordan transformation to spin variables σ_j ,

$$\alpha_j = \left(\prod_{k=1}^{j-1} \sigma_k^x \right) \sigma_j^z, \quad \beta_j = i \left(\prod_{k=1}^{j-1} \sigma_k^x \right) \sigma_j^z \sigma_j^x. \quad (8)$$

One obtains

$$\mathcal{H}_{\text{int}} = -g_1 \sum_j \sigma_j^x \sigma_{j+1}^x - g_2 \sum_j \sigma_j^z \sigma_{j+2}^z, \quad (9)$$

an interesting variant of the XY model, with nearest neighbor spin interactions along x and next nearest interactions along z . Adding direct hopping terms (assuming again a dimerized lattice) described by

$$\mathcal{H}_{\text{kin}} = it_1 \sum_j \alpha_j \beta_j + it_2 \sum_j \beta_j \alpha_{j+1} \quad (10)$$

gives, in the spin representation,

$$\mathcal{H}_{\text{kin}} = -t_1 \sum_j \sigma_j^x - t_2 \sum_j \sigma_j^z \sigma_{j+1}^z. \quad (11)$$

The full Hamiltonian $\mathcal{H} = \mathcal{H}_{\text{int}} + \mathcal{H}_{\text{kin}}$ is not exactly solvable for a general set of parameters but has several special points in the parameter space where exact solutions are known. These include an anisotropic XY model for $g_2 = t_1 = 0$ and a transverse field Ising model when $g_1 = t_2 = 0$ or when $g_1 = g_2 = 0$. A detailed exploration of the phase diagram of this model is beyond the scope of this study and we leave it to future work. It is clear, however, that the model exhibits a rich phase diagram with gapped and gapless phases, some of which are topologically non-trivial and carry unpaired Majorana zero modes at the edges.

Next we consider a *two-leg ladder* shown in Fig. 2b. The interacting Hamiltonian is given by the first term in Eq. (7). This model is exactly solvable for an arbitrary interaction strength g on the square plaquette. To see this note that each four-fermion term commutes with the Hamiltonian and is therefore a constant of motion. Furthermore, adding hopping t along the rung does not spoil the model's integrability, although hopping t' along the legs does. After the WJ transformation (8) the Hamiltonian can be written as $\mathcal{H} = \mathcal{H}_0 + \mathcal{H}'$ with

$$\mathcal{H}_0 = -g \sum_j \sigma_j^x \sigma_{j+1}^x - t \sum_j \sigma_j^x, \quad (12)$$

$$\mathcal{H}' = -t' \sum_j (\sigma_j^y \sigma_{j+1}^z + \sigma_j^z \sigma_{j+1}^y). \quad (13)$$

At the neutrality point ($t = t' = 0$) and assuming $g > 0$ the ground state is a doubly degenerate ferromagnet. In the fermion language this corresponds to complex fermions $c_j = \frac{1}{2}(\alpha_j + i\beta_j)$ on each rung either all occupied or all empty. Turning on $t \neq 0$ removes the two-fold degeneracy. Since this is a gapped state one expects it to be stable against the perturbation \mathcal{H}' as long as t' remains weak.

As a final 1D example we consider a *diamond chain* depicted in Fig. 2c. The interacting Hamiltonian is

$$\mathcal{H}_{\text{int}} = g_1 \sum_{j \text{ odd}} \gamma_j \alpha_j \beta_j \gamma_{j+1} + g_2 \sum_{j \text{ odd}} \gamma_{j+1} \alpha_{j+1} \beta_{j+1} \gamma_{j+2}, \quad (14)$$

where once again we allow for the possibility of dimerization. We observe that products $\alpha_j \beta_j$ commute with \mathcal{H}_{int} and with one another. They can thus be replaced by classical variables $is_j = \pm i$. The Hamiltonian becomes

$$\mathcal{H}_{\text{int}} = i \sum_{j \text{ odd}} (g_1 s_j \gamma_j \gamma_{j+1} + g_2 s_{j+1} \gamma_{j+1} \gamma_{j+2}), \quad (15)$$

describing a simple 1D chain with hoppings g_1 and g_2 between nearest neighbor sites. Because there are no closed loops in such a linear chain we can adopt a gauge in which $s_j = 1$ for all j . The Hamiltonian (15) then coincides with the Kitaev chain model³¹. Accordingly, its spectrum is gapped whenever $g_1 \neq g_2$. For an open ended chain with sites labeled $j = 1 \dots 2N$ the phase with $g_1 < g_2$ is topological and has unpaired Majorana zero modes bound to its two ends while $g_1 > g_2$ corresponds to the trivial phase. $g_1 = g_2$ marks the critical point separating the two phases. Adding \mathcal{H}_{kin} to the interacting Hamiltonian (14) spoils its integrability but again we may expect the gapped phases to be robust against small detuning from the neutrality point.

We now turn to 2D lattice geometries. A simple square lattice depicted in Fig. 2d is not exactly solvable and we shall discuss its phase diagram below. We consider first a modified square lattice shown in Fig. 2e which represents a somewhat artificial but exactly solvable 2D geometry with strong interactions. It is obtained by populating one sublattice with doubly quantized vortices each containing two exact Majorana zero modes α_j, β_j . The dominant interaction terms in this arrangement are of the form

$$\mathcal{H}_{\text{int}} = g \sum_{j, \nu} \alpha_j \beta_j \alpha_{j+\nu} \beta_{j+\nu} + g' \sum_{j, \delta_1, \delta_2} \alpha_j \beta_j \gamma_{j+\delta_1} \gamma_{j+\delta_2} \quad (16)$$

where $\delta = \pm \hat{x}, \pm \hat{y}$ are the nearest neighbor vectors while ν second neighbor vectors on the square lattice. The model is solvable because once again products $\alpha_j \beta_j$ commute with \mathcal{H}_{int} (and with one another) and can thus be replaced by classical variables $is_j = \pm i$. The resulting Hamiltonian is bilinear in the γ operators residing on the single vortex sites and can be analyzed in a straightforward fashion. Depending on the relative sign and amplitude of the couplings g and g' various phases are possible, including a gapless metallic phase when $g \gg g' > 0$ and, interestingly, dispersionless flat band at zero energy when $g < 0$ and $|g| \gg |g'|$. A detailed discussion of this model is given in appendix C.

A simple square lattice model Fig. 2d cannot be reduced to a non-interacting problem and we study it by a combination of approximate analytical techniques and by exact numerical diagonalization on small clusters. To facilitate the discussion we consider a dimerized situation

with couplings g_1 and g_2 on alternating rows of plaquettes, described by

$$\mathcal{H}_{\text{int}} = g_1 \sum_j \alpha_j \beta_j \alpha_{j+x} \beta_{j+x} + g_2 \sum_j \beta_j \alpha_{j-y} \beta_{j+x} \alpha_{j+x-y} \quad (17)$$

In the limit $g_2 = 0$ the system breaks up into a collection of two-leg ladders already discussed above. Assuming $g_1, g_2 \geq 0$ the exact ground state is a direct product of the ground states of the individual ladders. In the language of Ising spins defined in Eq. (8) these are doubly degenerate 1D ferromagnets. The ground state thus exhibits a 2^{N_y} -fold degeneracy, where N_y is the number of unit cells in the y direction. The spectrum of excitations is gapped and the lowest excited state at energy $2g_1$ has one of the spins reversed. Inclusion of nonzero g_2 can be seen to suppress the ferromagnetic order in the individual ladders by promoting excitations. A reasonable conjecture is that the gapped phase persists all the way to the isotropic point $g_2 = g_1$ which marks a quantum phase transition to another gapped state that is adiabatically connected to a set of independent ladders that occur at $g_1 = 0$.

We have performed a standard mean-field (MF) analysis by decoupling \mathcal{H}_{int} in all possible channels involving Majorana bilinears on nearest and next nearest neighbor bonds. At $g_2 = 0$ this procedure yields the exact ground state with $\Delta_1 = g_1 \langle i \alpha_j \beta_j \rangle = \pm g_1$ and all other order parameters zero. The two possible signs correspond to two degenerate ferromagnetic ground states on each ladder. Interestingly, this solution persists as the mean-field ground state for all values of $g_2 < g_1$. At $g_2 = g_1$ the MF theory predicts a strong first order transition to a state characterized by non-vanishing order parameter $\Delta_2 = g_2 \langle i \beta_j \alpha_{j-y} \rangle = \pm g_2$ which then persists all the way to $g_1 = 0$ where it becomes the exact ground state of \mathcal{H}_{int} . To ascertain the accuracy of the MF solution we carried out exact numerical diagonalizations (ED) of \mathcal{H}_{int} for a system containing $N_x \times 4$ lattice sites with N_x up to 19 (see appendix D). Some representative results are displayed in Fig. 3. These indicate that MF treatment provides a reasonable approximation for $g_2/g_1 \ll 1$ but breaks down when the two couplings are comparable. Specifically, ED indicates a continuous phase transition at $g_2 = g_1$ with the gap closing smoothly at that point.

We expect the gapped phases of the 2D model to remain robust against small detuning from the neutrality point. However, at the criticality, such detuning is likely to drive the system into another phase, adiabatically connected to the noninteracting system of Majorana fermions described by Hamiltonian (5). Our conjectured phase diagram describing this situation is displayed in Fig. 3e. The gapped phases in the interaction dominated regime are separated from the hopping dominated phases by topological phase transitions. This can be seen by analyzing the noninteracting Hamiltonian (5). It describes spinless fermions with charge conjugation symmetry. Since the time reversal symmetry is absent the

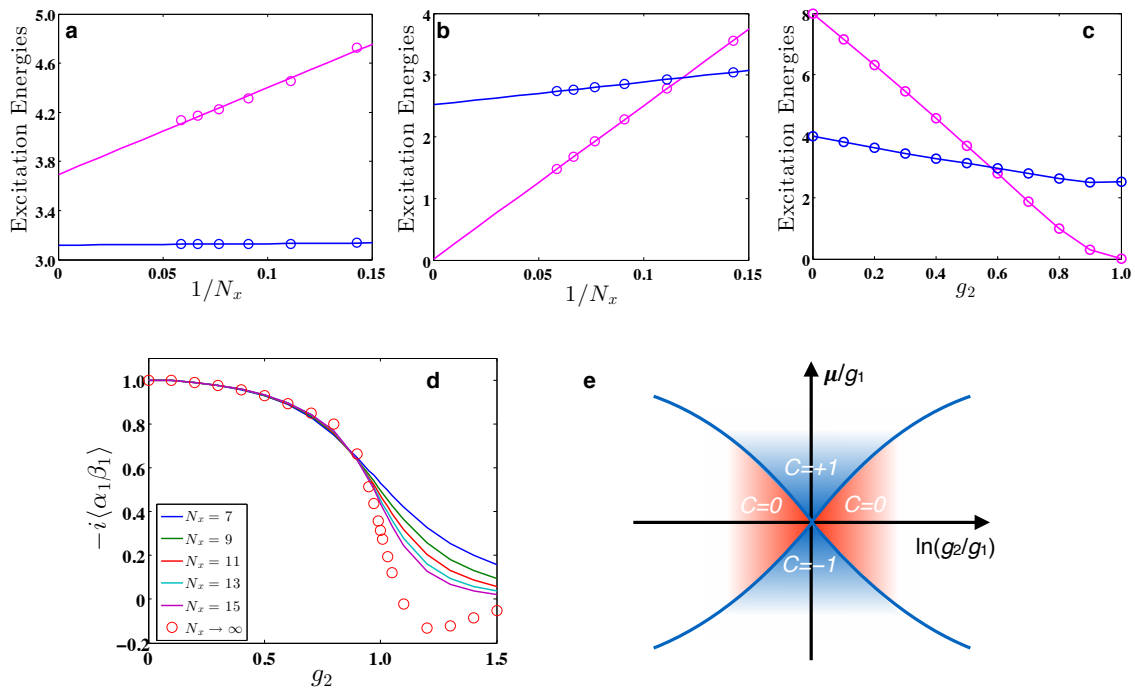


FIG. 3: Interacting system on the simple square lattice. Panels **a-c** show the finite size scaling analysis of the many-body excitation energies of the system obtained by exact numerical diagonalization. Energies of the two lowest excited states are shown as a function of $1/N_x$ for $g_2 = 0.5$ in **a** and $g_2 = 1.0$ in **b**. The excitation energies extrapolated to $N_x \rightarrow \infty$ are shown in panel **c** as a function of g_2 . Panel **d** shows the order parameter $\Delta_1 = -i\langle\alpha_1\beta_1\rangle$ as a function of g_2 for various system sizes. The infinite system extrapolation is obtained by assuming $\Delta_1 \simeq c_0 + c_1/N_x + c_2/N_x^2$. In panels **a-c** $g_1 = 1.0$ is held constant. **e** The schematic phase diagram for the simple square lattice system.

system is in topological class D which has integer classification in $d = 2$. Assuming that t_{ij} is dominated by first and second neighbor hoppings t and t' the system is gapped and one can easily calculate the corresponding Chern number $C = \text{sgn}(t^2 t') = \pm 1$. Assuming furthermore that for small chemical potential $t, t' \propto \mu$, as also shown in appendix A, we obtain $C = \text{sgn}(\mu)$, leading to the phase diagram illustrated in Fig. 3e. The interaction dominated phases by contrast are adiabatically connected to systems of decoupled two leg ladders and are thus topologically trivial with $C = 0$.

IV. OUTLOOK

When the chemical potential is tuned to coincide with the Dirac point in the superconducting surface of a strong topological insulator Majorana fermions bound to the vortex cores show a completely flat band, protected by the chiral symmetry. In this regime the nature of the ground state is determined by interactions between the Majorana zero modes and the system must be regarded as inherently strongly correlated. We gave examples of lattice geometries in one and two dimensions for which the ground state of the strongly interacting system can be found exactly. In other cases, such as the simple 1D Majorana chain, exact solution of the interacting problem is

unknown but the Hamiltonian maps onto an interesting spin problem which can be studied by standard techniques such as the density matrix renormalization group (DMRG). Although well understood theoretically spin models in 1D often face significant hurdles when it comes to experimental realizations. For instance the fine details of quantum criticality in the transverse field Ising model – perhaps the most widely studied 1D spin model – have been only recently mapped out experimentally³⁴. Our construction may thus enable new experimental realizations of these well studied models. The simple square lattice in 2D shows an interesting phase diagram with both topological and trivial gapped phases as well as a quantum phase transition that cannot be described by mean field theory. Further interesting phases in 2D may arise in lattices with triangular symmetry which we have not considered in this study.

The ultimate goal of these constructions is to find novel phases that cannot be adiabatically deformed into phases of weakly interacting fermions. With the notable exception of the simple 1D Majorana chain (some of whose ground states are likely to be Luttinger liquids) we have not thus far succeeded in identifying such strongly interacting phases. We note, however, that Majorana interactions of the form Eq. (1) play a pivotal role in the construction of various “interaction enabled” topological phases introduced in the seminal work by Fidkowski

and Kitaev³². Our work indicates how such interactions can be generated and controlled in a system that is now physically accessible thanks to the recent experimental breakthroughs^{11–17,19}. More recently, a specific model has been formulated by Lapa, Teo and Hughes³³ that produces an interaction enabled topological crystalline phase (which has no analog in a weakly interacting system) and also employs Majorana interaction of the type discussed in this work as the key component. We are optimistic that such a phase can be engineered using our insight and experimental ingredients that are presently available.

V. ACKNOWLEDGMENT

The authors thank I. Affleck, J. Alicea, T. Liu, A. Rahmani, G. Refael, K. Shtengel and X. Zhu for useful discussions. The authors are indebted to NSERC, CIFAR and Max Planck - UBC Centre for Quantum Materials for support. M.F. acknowledges The Aspen Center for Physics and IQMI at Caltech for hospitality during various stages of this project.

Appendix A: Zero modes in Fu-Kane model

Fu and Kane¹⁸ envisioned inducing superconductivity in the surface state of a 3D topological insulator by covering it in with a thin film of an ordinary s -wave superconductor such as Pb or Nb. The resulting second-quantized Hamiltonian describing the surface state can be written as

$$\mathcal{H} = \int d^2r \hat{\Psi}_r^\dagger H_{FK}(\mathbf{r}) \hat{\Psi}_r, \quad (\text{A1})$$

where $\hat{\Psi}_r = (c_{\uparrow r}, c_{\downarrow r}, c_{\downarrow r}^\dagger, -c_{\uparrow r}^\dagger)^T$ is the Nambu spinor and

$$H_{FK}(\mathbf{r}) = \begin{pmatrix} -\mu & p_- & \Delta(\mathbf{r}) & 0 \\ p_+ & -\mu & 0 & \Delta(\mathbf{r}) \\ \Delta^*(\mathbf{r}) & 0 & \mu & -p_- \\ 0 & \Delta^*(\mathbf{r}) & -p_+ & \mu \end{pmatrix}, \quad (\text{A2})$$

where $p_\pm = p_x \pm ip_y$, and we have set $v = 1$ and μ is the chemical potential. The diagonal blocks describe the kinetic energy of the STI surface state (single Dirac fermion) while the off-diagonal blocks encode the SC pair potential.

As the first step we are interested in finding the eigenstates $\Phi_n(\mathbf{r})$ of $H_{FK}(\mathbf{r})$ in the presence of a single Abrikosov vortex. For a vortex placed at the origin we write

$$\Delta(\mathbf{r}) = \Delta_0(r) e^{-i(n\varphi + \theta)}, \quad (\text{A3})$$

where $\Delta_0(r)$ is a real function of the distance, φ represents the polar angle and θ denotes an arbitrary constant

phase offset due to other vortices that could be present in the system far away from the origin. Integer n denotes the vorticity. Single-valuedness of the Hamiltonian dictates that $\Delta_0(r)$ vanishes at the origin. Energy considerations further show that $\Delta_0(r) \sim r^{|n|}$ for small r .

To find the zero modes of $H_{FK}(\mathbf{r})$ in the presence of a vortex it is useful to first perform a unitary transformation $\tilde{H}_{FK} = U H_{FK} U^{-1}$ with

$$U = \begin{pmatrix} 1 & 0 & 0 & 0 \\ 0 & 0 & 0 & 1 \\ 0 & 0 & 1 & 0 \\ 0 & 1 & 0 & 0 \end{pmatrix}, \quad (\text{A4})$$

which brings the Hamiltonian into the following form

$$\tilde{H}_{FK} = \begin{pmatrix} M & D \\ D^\dagger & -M \end{pmatrix}, \quad D = \begin{pmatrix} \Delta(\mathbf{r}) & p_- \\ -p_+ & \Delta^*(\mathbf{r}) \end{pmatrix}. \quad (\text{A5})$$

and $M = \text{diag}(-\mu, \mu)$. The transformed Hamiltonian acts on the modified Nambu spinor $\tilde{\Psi}_r = (c_{\uparrow r}, -c_{\uparrow r}^\dagger, c_{\downarrow r}^\dagger, c_{\downarrow r})^T$. Passing into the polar coordinates and making use of the identity $p_\pm = e^{\pm i\varphi}(-i\partial_r \pm r^{-1}\partial_\varphi)$ we may write

$$D = \begin{pmatrix} e^{-i(n\varphi + \theta)} \Delta_0(r) & e^{-i\varphi}(-i\partial_r - \frac{\partial_\varphi}{r}) \\ -e^{i\varphi}(-i\partial_r + \frac{\partial_\varphi}{r}) & e^{i(n\varphi + \theta)} \Delta_0(r) \end{pmatrix}. \quad (\text{A6})$$

We now temporarily focus on the neutrality point where $M = 0$ and the Hamiltonian (A5) is purely off-diagonal. When looking for the zero modes the off-diagonal form has a distinct advantage: the zero modes necessarily have the spinor structure $(\psi(\mathbf{r}), 0)^T$ and $(0, \chi(\mathbf{r}))^T$ where $\psi(\mathbf{r})$ and $\chi(\mathbf{r})$ are two-component zero modes of D^\dagger and D respectively. For a singly quantized vortex ($n = 1$) it is easy to show that there exists a normalizable zero mode of D of the form

$$\chi_0(\mathbf{r}) = \frac{1}{\sqrt{2}} \begin{pmatrix} e^{-i(\theta/2 - \pi/4)} \\ e^{i(\theta/2 - \pi/4)} \end{pmatrix} f_0(r), \quad (\text{A7})$$

with $f_0(r) = A e^{-\int_0^r \Delta_0(r') dr'}$, while D^\dagger does not have a normalizable zero mode. The field operator of the zero mode reads

$$\gamma = \frac{i}{\sqrt{2}} \int d^2r \left[e^{i(\theta/2 - \pi/4)} c_{r\downarrow} - e^{-i(\theta/2 - \pi/4)} c_{r\downarrow}^\dagger \right] f_0(r). \quad (\text{A8})$$

As expected, the zero mode represents a Majorana particle, $\gamma^\dagger = \gamma$. For $\mu \neq 0$ the structure of the zero mode wavefunction becomes slightly more complicated²¹; in addition to the exponential decay it exhibits an oscillatory behavior $\sim \sin kr$ where k is a wavevector close to the Fermi wavevector k_F .

Now consider two vortices located at points \mathbf{R}_1 and \mathbf{R}_2 , such that $|\mathbf{R}_1 - \mathbf{R}_2| \gg \xi$. The two-vortex Hamiltonian $H_{FK}^{(2)}$ still has the structure displayed in Eq. (A5) except that $\Delta(\mathbf{r})$ now encodes vortices at \mathbf{R}_1 and \mathbf{R}_2 . We can seek its low-energy eigenstates in the basis spanned

by the zero mode wavefunctions $\Phi_1(\mathbf{r}) = (0, \chi_0(\mathbf{r} - \mathbf{R}_1))^T$ and $\Phi_2(\mathbf{r}) = (0, \chi_0(\mathbf{r} - \mathbf{R}_2))^T$. If we denote the two Majorana operators as γ_1 and γ_2 then the zero mode splitting comes from the term $t_{12}\gamma_1\gamma_2$ with the overlap integral $t_{12} = \langle \Phi_1 | H_{\text{FK}}^{(2)} | \Phi_2 \rangle$. At the neutrality point the matrix element t_{12} trivially evaluates to zero because $|\Phi_1\rangle$ is orthogonal to $H_{\text{FK}}^{(2)}|\Phi_2\rangle$ for arbitrary positions \mathbf{R}_1 and \mathbf{R}_2 . The zero modes therefore remain exact. Away from the neutrality point we obtain

$$\begin{aligned} t_{12} &= \int d^2r \chi_0^\dagger(\mathbf{r} - \mathbf{R}_1) (-M) \chi_0(\mathbf{r} - \mathbf{R}_2) \quad (\text{A9}) \\ &= i\mu \sin\left(\frac{\theta_1 - \theta_2}{2}\right) F_{12} \end{aligned}$$

with $F_{12} = \int d^2r f_0(\mathbf{r} - \mathbf{R}_1) f_0(\mathbf{r} - \mathbf{R}_2)$; the overlap is proportional to μ and is generally nonzero.

Appendix B: Interaction terms

We now wish to consider the four-fermion terms that will arise from Coulomb or possibly other interactions present in the solid. Suppose we have solved the single-electron problem in the presence of N vortices. We thus have the complete set of eigenfunctions $\Phi_n(\mathbf{r})$ and eigenenergies E_n of $H_{\text{FK}}^{(N)}$. The second quantized Hamiltonian (A1) can then be written in a diagonal form $\mathcal{H} = \sum_n E_n \hat{\psi}_n^\dagger \hat{\psi}_n + E_g$ where

$$\hat{\psi}_n = \int d^2r \Phi_n^\dagger(\mathbf{r}) \hat{\Psi}_r \quad (\text{B1})$$

are the eigenmode operators. The sum over n is restricted to the positive energy eigenvalues and E_g is a constant representing the ground state energy. At the neutrality point, according to our preceding discussion, N of the $\hat{\psi}_n$ eigenmodes coincide with the exact zero modes belonging to the individual vortex cores. We denote these γ_j with $j = 1 \dots N$.

The Coulomb interaction, appropriately screened, can be written as

$$U = \frac{1}{2} \int \int d^2r d^2r' \hat{\rho}(\mathbf{r}) V(\mathbf{r} - \mathbf{r}') \hat{\rho}(\mathbf{r}'), \quad (\text{B2})$$

where $V(\mathbf{r})$ is the interaction potential and $\hat{\rho}(\mathbf{r}) = c_{\sigma\mathbf{r}}^\dagger c_{\sigma\mathbf{r}}$ is the charge density operator. The latter can be expressed in terms of modified Nambu spinors as $\hat{\rho}(\mathbf{r}) = \hat{\Psi}_r^\dagger O_\rho \hat{\Psi}_r$ with $O_\rho = \frac{1}{2} \text{diag}(1, -1, -1, 1)$. Next, by exploiting the completeness of the eigenstates $\Phi_n(\mathbf{r})$ we can invert Eq. (B1) to obtain

$$\hat{\Psi}_r = \sum_n \Phi_n(\mathbf{r}) \hat{\psi}_n \quad (\text{B3})$$

and express the charge density in terms of the eigenmode operators as

$$\hat{\rho}(\mathbf{r}) = \sum_{n,m} [\Phi_n^\dagger(\mathbf{r}) O_\rho \Phi_m(\mathbf{r})] \hat{\psi}_n^\dagger \hat{\psi}_m. \quad (\text{B4})$$

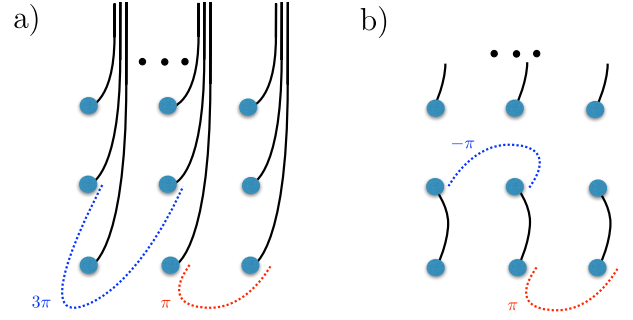


FIG. 4: Phase difference counting in the vortex lattice. The phase θ_j of the vortex j is defined to the right of its core. Because $\theta_j/2$ is required to calculate the density in Eq. (B7) we must keep track of branch cuts emanating from the vortex cores. **a** Examples of the branch cuts and the resulting phase differences between the vortices. **b** The branch cuts from panel **a** may be connected at infinity and contracted to form finite cuts between the adjacent vortices. The phase differences stay the same modulo 4π , which does not alter the density.

Substituting this result into Eq. (B2) and projecting onto the zero mode subspace we arrive at the interaction between Majorana modes of the form

$$U_0 = \frac{1}{2} \sum_{ijkl} \gamma_i \gamma_j \gamma_k \gamma_l \int \int d^2r d^2r' \rho_{ij}(\mathbf{r}) V(\mathbf{r} - \mathbf{r}') \rho_{kl}(\mathbf{r}'), \quad (\text{B5})$$

where

$$\rho_{ij}(\mathbf{r}) = [\Phi_i^\dagger(\mathbf{r}) O_\rho \Phi_j(\mathbf{r})]. \quad (\text{B6})$$

At the neutrality point we can use Eq. (A7) to write

$$\rho_{ij}(\mathbf{r}) = -\frac{i}{2} \sin\left(\frac{\theta_i - \theta_j}{2}\right) f_0(\mathbf{r} - \mathbf{R}_i) f_0(\mathbf{r} - \mathbf{R}_j). \quad (\text{B7})$$

Noting the antisymmetry $\rho_{ij}(\mathbf{r}) = -\rho_{ji}(\mathbf{r})$, the expression for the interaction parameter g defined in Eq. (4) of the main text can be simplified, for the group of four Majoranas $\gamma_1 \dots \gamma_4$, as

$$g = 4(g_{1234} + g_{4123} - g_{1324}). \quad (\text{B8})$$

The three distinct terms can now be evaluated with the help of Eq. (B7). An especially simple form arises if we assume that the interaction is well screened so that it is essentially point-like on the scale set by the SC coherence ξ , i.e. $V(\mathbf{r}) = V_0 \delta(\mathbf{r})$. For a square arrangement of vortices we notice the phase difference structure of the lattice shown in Fig. 4. The structure is consistent with the one obtained in³⁰. We then obtain $g_{\square} = -2V_0 F_{1234}$ where $F_{1234} = \int d^2r \prod_{j=1}^4 f_0(\mathbf{r} - \mathbf{R}_j)$. For a linear arrangement of the four vortices one similarly obtains $g_{-} = -V_0 F_{1234}$.

Appendix C: Exactly solvable 2D model

The building block for the solvable Majorana model in 2D is a doubly quantized vortex defined by Eq. (A3) with

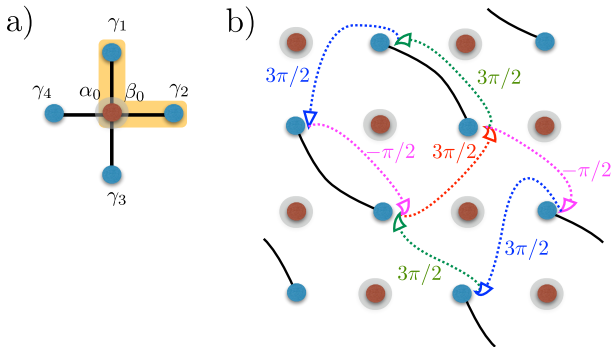


FIG. 5: Modified square lattice structure **a** A site with the doubly quantized vortex surrounded by singly quantized vortices. The dominant type of interaction within such a node is shaded in yellow. **b** Phase difference structure for a choice of gauge in the modified square lattice.

($n = 2$). The solution for the Majorana wavefunction goes along similar lines as for the single vortex²⁸. We search for zero mode solutions of operator D defined in Eq. (A6) with $n = 2$ in the form

$$\chi_m(\mathbf{r}) = \frac{1}{\sqrt{2}} \begin{pmatrix} e^{i((1-m)\varphi + \theta/2 - \pi/4)} u_m(r) \\ e^{-i(m\varphi + \theta/2 - \pi/4)} v_m(r) \end{pmatrix}. \quad (\text{C1})$$

We substitute this into D to obtain

$$\begin{cases} \Delta_0(r)u_m(r) + (\partial_r - \frac{m}{r})v_m(r) = 0, \\ \Delta_0(r)v_m(r) + (\partial_r - \frac{1-m}{r})u_m(r) = 0. \end{cases} \quad (\text{C2})$$

It is known²⁸ that these equations have normalizable real solutions for $m = 0, 1$, for which it holds

$$u_1 = v_0, \quad v_1 = u_0. \quad (\text{C3})$$

This observation allows us to write the field operator of the zero modes

$$\begin{aligned} \alpha(\mathbf{r}) &\propto [e^{i(\varphi + \theta/2 - \pi/4)} c_{\mathbf{r}\downarrow} + e^{-i(\varphi + \theta/2 - \pi/4)} c_{\mathbf{r}\downarrow}^\dagger] u_0(r) \\ &\quad + [e^{i(\theta/2 - \pi/4)} c_{\mathbf{r}\downarrow} + e^{-i(\theta/2 - \pi/4)} c_{\mathbf{r}\downarrow}^\dagger] v_0(r), \quad (\text{C4}) \\ \beta(\mathbf{r}) &\propto i[e^{i(\varphi + \theta/2 - \pi/4)} c_{\mathbf{r}\downarrow} - e^{-i(\varphi + \theta/2 - \pi/4)} c_{\mathbf{r}\downarrow}^\dagger] u_0(r) \\ &\quad - i[e^{i(\theta/2 - \pi/4)} c_{\mathbf{r}\downarrow} - e^{-i(\theta/2 - \pi/4)} c_{\mathbf{r}\downarrow}^\dagger] v_0(r). \end{aligned}$$

It is easy to show that the density is then given by

$$\rho_{\alpha\beta} \propto [u_0^2(r) - v_0^2(r)]. \quad (\text{C5})$$

This expression depends only on the distance from the vortex core. It decays exponentially on distances longer than the coherence length ξ .

We are now interested in the dominant interactions between the Majoranas in such a model. For this we notice that the interaction is the largest for the combinations $g\alpha_j\beta_j\alpha_{j+\nu}\beta_{j+\nu}$ and $g'\alpha_j\beta_j\gamma_{j+\delta_1}\gamma_{j+\delta_2}$ depending on how strong the screening of the Coulomb interactions is. The corresponding interaction strengths are proportional to $\exp[-|\mathbf{R}_{j+\nu} - \mathbf{R}_j|/R_c]$,

where R_c is the Coulomb screening length, and $\exp[-(|\mathbf{R}_j - \mathbf{R}_{j+\delta_1}| + |\mathbf{R}_j - \mathbf{R}_{j+\delta_2}|)/\xi]$.

Consider first the case $R_c < \xi$. The dominant interaction is the g' term as Coulomb interaction on long length-scale decays faster than the overlap of the Majorana wavefunctions. This interaction term dominates as it does not involve the smallness due to the screening of the Coulomb interaction, only due to the decay of the Majorana wavefunctions. Following the observation of the previous section that $\rho_{ij} \propto \sin((\theta_i - \theta_j)/2)$, we see that the interaction is proportional to $\sin((\theta_{j+\delta_1} - \theta_{j+\delta_2})/2)$. This is the interaction of the form $\rho_{\alpha\beta}\rho_{\gamma\gamma}$. The rest of the terms in (B8) are canceling each other, since α_j and β_j are different by as if they had a phase difference π .

As we noted in the main text, the products $i\alpha_j\beta_j$ commute with the Hamiltonian and with each other. Thus they are conserved quantities $s_j = \pm 1$ signaling the occupation of the Andreev states $c_j = \frac{1}{2}(\alpha_j + i\beta_j)$. This means that we can trace out these degrees of freedom from the model and obtain the hopping amplitudes between the single-vortex sites. The relevant phase differences θ are depicted in Fig. 5b. We consider two possible configurations of s_j : ferromagnetic (all +1 or all -1) and antiferromagnetic (staggered on the two sublattices). It is easy to see that for the FM configuration the hopping amplitudes on a given bond contributed by the two adjacent double vortex sites add up while for the AF configuration they cancel. Therefore, in the FM case the resulting hopping model produces a completely flat Majorana band. Meanwhile for the AF configuration the hopping model will be of the form indicated in Eq. (5) of the main text with the nearest neighbor hopping $t = 2g'$. The energy spectrum then consists of a pair of dispersing bands with energies

$$E_{\mathbf{k}} = \pm 4g' \sqrt{\sin^2\left(\frac{k_x + k_y}{2}\right) + \sin^2\left(\frac{k_x - k_y}{2}\right)} \quad (\text{C6})$$

where \mathbf{k} ranges over the reduced Brillouin zone. Occupying the negative energy states in Eq. (C6) clearly produces lower ground state energy than occupying a flat band at zero energy and therefore the FM state will be the stable ground state of the system. For the screened Coulomb interaction, therefore, a gapless metallic phase with the excitation spectrum (C6) is produced.

Now consider the case $R_c > \xi$. Here the dominant interaction is between the double vortices. If the interaction is the usual Coulomb repulsion, $g \gg g' > 0$, then the preferred occupation s_j of the double vortices is antiferromagnetic and the hopping model obtained is the flat Majorana band, as discussed above. Smaller terms involving four single vortex sites can split this degeneracy, but the model thus obtained is not integrable. If the interaction is attractive, $g < 0$, $|g| \gg |g'|$, then the preferred occupation of the double vortices is ferromagnetic and the resulting model is the same as for the screened Coulomb, a gapless dispersing Majorana band Eq. (C6).

Appendix D: 2D single Majorana vortex lattice

The exact diagonalization study of the system on the simple square lattice is performed by transforming the Hamiltonian (17) to the fermionic basis, $\alpha_j = c_j^\dagger + c_j$, $\beta_j = i(c_j^\dagger - c_j)$. The Hamiltonian then becomes

$$\begin{aligned} \mathcal{H}_{\text{int}} = & -g_1 \sum_j (2N_j - 1)(2N_{j+x} - 1) \\ & + g_2 \sum_j (c_j^\dagger - c_j)(c_{j+x}^\dagger - c_{j+x}) \\ & \times (c_{j-y}^\dagger + c_{j-y})(c_{j-y+x}^\dagger + c_{j-y+x}) \end{aligned} \quad (\text{D1})$$

where $N_j = c_j^\dagger c_j$ denotes the number operator and \mathbf{j} indicates the 2D coordinate (n, m) of the unit cell. If we were to directly diagonalize the many-body Hamiltonian, only a small system can be numerically treated. Fortunately, \mathcal{H}_{int} can be block-diagonalized by defining the fermion parity operators

$$\hat{F}_n^x = (-1)^{\sum_m N_{n,m}}, \quad \hat{F}_m^y = (-1)^{\sum_n N_{n,m}}, \quad (\text{D2})$$

which commute with the Hamiltonian \mathcal{H}_{int} and among themselves. Their eigenvalues (± 1) are good quantum numbers and label the different blocks of the Hamiltonian. However, these operators are not independent since they are connected by the total fermionic parity operator $\hat{F} = \prod_n \hat{F}_n^x = \prod_m \hat{F}_m^y$.

We consider separately the cases when the number N_x of unit cells in the x direction is odd and even. The Hamiltonian can be easily block-diagonalized by $F_n^x = \pm 1$ and $F_m^y = \pm 1$. We are able to numerically solve the block-diagonalized Hamiltonian for a system containing $N_x \times 4$ unit cells with N_x up to 19 as follows. We first find one of the degenerate ground states $|G\rangle$ in the parity sector $F_n^x = 1$ and $F_m^y = 1$ for all n and m . We then use the operator $\hat{A}_{\tilde{m}} = \prod_n \alpha_{n,\tilde{m}}$ to generate the remaining ground states. Note that $\hat{A}_{\tilde{m}}$ commutes with \mathcal{H}_{int} but anticommutes with all \hat{F}_n^x . When it acts on a ground state it thus flips the sign of all F_n^x generating a new ground state in a different parity sector.

When we subsequently apply $\hat{A}_{\tilde{m}'}$ with $\tilde{m}' \neq \tilde{m}$ to this new ground state all F_n^x flip back. This construction indicates that there exist *at least* two degenerate ground states. For even N_x , our numerical results support the two-fold ground state degeneracy. For odd N_x , $\hat{A}_{\tilde{m}}$ also flips the sign of F_m^y . Since the number of \hat{F}_m^y operators is N_y and $F_m^y = \pm 1$ the degenerate ground states are given by

$$|F_{\tilde{m}_\pm}^y = \pm 1\rangle = \prod_{\tilde{m}_-} \hat{A}_{\tilde{m}_-} |G\rangle. \quad (\text{D3})$$

It follows that the number of the degenerate ground states is *at least* 2^{N_y} . This agrees with the degeneracy that occurs in the extreme anisotropy limit $g_2 = 0$, already discussed in the main text.

Interestingly, the systems with even and odd N_x exhibit different physical properties even in the thermodynamic limit. When N_x is even, by performing a Z_2 gauge transformation $\alpha_{2l,m} \rightarrow -\alpha_{2l,m}$, the Hamiltonian \mathcal{H}_{int} changes the sign. That is, when the many-body state has energy E , the state after the gauge transformation has energy $-E$. This many-body version of the particle-hole symmetry shows that $g_1, g_2 \geq 0$ describes identical physics as $g_1, g_2 \leq 0$. However, for odd N_x , $\alpha_{2l,m} \rightarrow -\alpha_{2l,m}$ does not simply flip the sign of \mathcal{H}_{int} due to the frustration at the boundary with the periodic boundary condition. Hence, systems with positive g_1 and g_2 are different from those with negative g_1 and g_2 in this case.

After obtaining the many-body wavefunctions of the ground states from the exact diagonalization, the order parameter $\Delta_1 = -i\langle \alpha_j \beta_j \rangle$ can be computed as a ground state expectation value in different parity sectors. We mainly focus on odd N_x . Because $\hat{A}_{\tilde{m}} = \prod_n \alpha_{n,\tilde{m}}$ connects the ground states in the different parity sectors, $\Delta_1 j$ must be computed in only one of the parity sectors, say $F_n^x = 1$ and $F_m^y = 1$ for all \tilde{n} and \tilde{m} , as shown in Fig. 3d. The expectation value flips the sign when we consider the ground state with parity $F_m^y = -1$.

¹ D.C. Tsui, H.L. Stormer, and A.C. Gossard, Phys. Rev. Lett. **48**, 1559 (1982).

² R.B. Laughlin, Phys. Rev. Lett. **50**, 1395 (1983).

³ E. Tang, J.-W. Mei and X.-G. Wen, Phys. Rev. Lett. **106**, 236802 (2011).

⁴ K. Sun, Z. Gu, H. Katsura and S. Das Sarma, Phys. Rev. Lett. **106**, 236803 (2011).

⁵ T. Neupert, L. Santos, C. Chamon and C. Mudry, Phys. Rev. Lett. **106**, 236804 (2011).

⁶ X. Hu, M. Kargarian and G. Fiete, Phys. Rev. B **84** 155116 (2011).

⁷ D.N. Sheng, Z.-C. Gu, K. Sun, and L. Sheng, Nat. Comm.

2, 389 (2011).

⁸ N. Regnault, B.A. Bernevig, Phys. Rev. X **1**, 021014 (2011).

⁹ Nigel R. Cooper and Jean Dalibard Phys. Rev. Lett. **110** 185301 (2013).

¹⁰ N. Y. Yao, A. V. Gorshkov, C. R. Laumann, A. M. Lauchli, J. Ye, and M. D. Lukin Phys. Rev. Lett. **110** 185302 (2013)

¹¹ G. Koren, T. Kirzhner, E. Lahoud, K. B. Chashka, and A. Kanigel, Phys. Rev. B **84**, 224521 (2011).

¹² L. Zhao, H. Deng, I. Korzhovska, J. Secor, M. Begliar-bekov, Z. Chen, E. Andrade, E. Rosenthal, A. Pasupathy, V. Oganesyan, and L. Krusin-Elbaum, arXiv:1408.1046.

- ¹³ B. Sacépé, J. B. Oostinga, J. Li, A. Ubaldini, N. J. G. Couto, E. Giannini, and A. F. Morpurgo, *Nat. Comm.* **2**, 575 (2011).
- ¹⁴ F. Qu, F. Yang, J. Shen, Y. Ding, J. Chen, Z. Ji, G. Liu, J. Fan, X. Jing, C. Yang, and Li Lu, *Scientific Reports* **2**, 339 (2012).
- ¹⁵ J. R. Williams, A. J. Bestwick, P. Gallagher, S. S. Hong, Y. Cui, A. S. Bleich, J. G. Analytis, I. R. Fisher, and D. Goldhaber-Gordon, *Phys. Rev. Lett.* **109**, 056803 (2012).
- ¹⁶ S. Cho, B. Dellabetta, A. Yang, J. Schneeloch, Z. Xu, T. Valla, G. Gu, M. J. Gilbert, and N. Mason, *Nat. Comm.* **4**, 1689 (2013).
- ¹⁷ S.-Y. Xu, N. Alidoust, I. Belopolski, A. Richardella, C. Liu, M. Neupane, G. Bian, S.-H. Huang, R. Sankar, C. Fang, B. Dellabetta, W. Dai, Q. Li, M. J. Gilbert, F. Chou, N. Samarth, and M. Zahid Hasan, arXiv:1410.5405.
- ¹⁸ L. Fu and C. L. Kane, *Phys. Rev. Lett.* **100**, 096407 (2008).
- ¹⁹ J.-P. Xu, C. Liu, M.-X. Wang, J. Ge, Z.-L. Liu, X. Yang, Y. Chen, Y. Liu, Z.-A. Xu, C.-L. Gao, D. Qian, F.-C. Zhang, and J.-F. Jia, *Phys. Rev. Lett.* **112**, 217001 (2014).
- ²⁰ M. Cheng, R. M. Lutchyn, V. Galitski, and S. Das Sarma, *Phys. Rev. Lett.* **103**, 107001 (2009).
- ²¹ M. Cheng, R. M. Lutchyn, V. Galitski, and S. Das Sarma, *Phys. Rev. B* **82**, 094504 (2010).
- ²² Y. E. Kraus and A. Stern, *New J. Phys.* **13** 105006 (2011).
- ²³ J. Zhou, Y.-J. Wu, R.-W. Li, J. He, and S.-P. Kou, *Europhys. Lett.* **102**, 47005 (2013).
- ²⁴ M. A. Silaev, *Phys. Rev. B* **88**, 064514 (2013).
- ²⁵ R. R. Biswas, *Phys. Rev. Lett.* **111**, 136401 (2013).
- ²⁶ J.C.Y. Teo and C.L. Kane, *Phys. Rev. B* **82**, 115120 (2010).
- ²⁷ Fu-Kane model at the neutrality point coincides with the Jackiw-Rossi model well known in particle physics²⁸. An index theorem for Dirac fermions applied to this model²⁹ is known to connect the total vorticity with the number of protected fermionic zero modes. This property of the Fu-Kane model was previously noted in Ref.²¹.
- ²⁸ R. Jackiw and P. Rossi, *Nucl. Phys. B* **190**, 681 (1981).
- ²⁹ E.J. Weinberg, *Phys. Rev. D* **24**, 2669 (1981).
- ³⁰ E. Grosfeld and A. Stern, *Phys. Rev. B* **73**, 201303(R) (2006).
- ³¹ A.Y. Kitaev, *Phys. Usp.* **44**, 131 (2001).
- ³² L. Fidkowski and A. Kitaev, *Phys. Rev. B* **81**, 134509 (2010).
- ³³ M.F. Lapa, J.C.Y. Teo and T.L. Hughes, arXiv:1409.1234.
- ³⁴ R. Coldea, D. A. Tennant, E. M. Wheeler, E. Wawrzynska, D. Prabhakaran, M. Telling, K. Habicht, P. Smeibidl, and K. Kiefer, *Science* **327**, 177 (2010).